Inverted L-Arm Gripper Compliant Mechanism

Jason Dearden
Compliant Mechanisms Research Group,
Department of Mechanical Engineering,
Brigham Young University,
Provo, UT 84602

Clayton Grames
New Product Development,
Intuitive Surgical, Inc.,
Sunnyvale, CA 94086

Brian D. Jensen
Department of Mechanical Engineering,
Brigham Young University,
Provo, UT 84602

Spencer P. Magleby
Department of Mechanical Engineering,
Brigham Young University,
Provo, UT 84602

Larry L. Howell[1]
Department of Mechanical Engineering,
Brigham Young University,
Provo, UT 84602
e-mail: lhowell@byu.edu

This work exploits the advantages of compliant mechanisms (devices that achieve their motion through the deflection of flexible members) to enable the creation of small instruments for minimally invasive surgery (MIS). Using flexures to achieve motion presents challenges, three of which are considered in this work. First, compliant mechanisms generally perform inadequately in compression. Second, for a ±90 deg range of motion desired for each jaw, the bending stresses in the flexures are prohibitive considering materials used in current instruments. Third, for cables attached at fixed points on the mechanism, the mechanical advantage will vary considerably during actuation. Research results are presented that address these challenges using compliant mechanism principles as demonstrated in a two-degree-of-freedom (2DoF) L-Arm gripper. [DOI: 10.1115/1.4036336]

Keywords: compliant mechanism, minimally invasive surgery, surgical instrument, nitinol

1 Introduction

Minimally invasive surgery (MIS), an alternative to traditional surgery, has several benefits including less patient trauma, decreased procedure time, and little to no scarring due to the small size of the incisions [1]. As advances in MIS are made, these potential benefits will become more apparent and procedures not previously possible will become more feasible. One way to advance MIS is to scale instruments to smaller sizes, thus facilitating smaller incisions and more intricate procedures. Current instruments present some issues when scaled to smaller sizes, including in their design and manufacturing. As the size of MIS instruments is decreased, new methods are needed to retain or increase instrument range of motion and performance.

The use of compliant mechanisms in minimally invasive surgery devices is attractive for reasons that include an ability to scale designs, reduce or even eliminate assembly, assure precise motion, and reduce part count, friction, and wear [2]. The motivation for this research is to demonstrate the use of compliant mechanisms in robotic MIS instruments, specifically to achieve end-effector wrist and gripper motion.

Although compliant mechanisms show promise for advancements in minimally invasive surgery, three challenges accompany their development for use in grippers:

(1) Preload in cable-actuated systems induces compressive loads on components, but compliant members generally perform inadequately in compression [3].
(2) For the ±90 deg range of motion desired for each jaw, the resulting bending stresses in the flexures are too high for materials used in current instruments.
(3) The moment arm for cables attached at fixed points on the mechanism will result in a changing and diminishing mechanical advantage during actuation.

These challenges are considered while exploring the geometry, strain–deflection relationship, and possible manufacturing methods for a two-degree-of-freedom gripper compliant mechanism. A large-scale prototype with a 38-mm diameter shaft was created to demonstrate mechanism functionality. A 6-mm diameter prototype was also created. Finite element (FE) analysis was used to determine the strain–deflection relationship of the flexures for a 3-mm device.

Research has been conducted regarding the application of compliant mechanisms in minimally invasive surgery, including MIS wrist mechanisms. A review of wrist mechanisms is found in Ref. [4]. Compliant designs include a superelastic NiTi wrist [5], an asymmetric wrist [6], and a virtual center compliant MIS tool [7]. Compliant end-effector designs include an endoscopic suturing device [8], a statically balanced surgical grasper [9], a force-limiting scalpel [10], and the origami-inspired compliant forceps, the Oriceps [11].

2 Inverted L-Arm Concept

The L-Arm gripper mechanism concept was developed to demonstrate the feasibility of overcoming the three challenges in this context associated with compliant mechanisms noted earlier: inadequate performance in compression, high stresses induced while under large deformations, and a mechanical advantage that varies as a function of deflection. The flexure-based L-Arm gripper is a compliant mechanism composed of two opposing L-shaped grippers with flexures that enable each of the jaws to actuate independently as shown in Fig. 1(*a*). The L-Arm gripper shows promise due to the simplicity of the mechanism and the possibility to increase performance over current mesoscale instruments, including larger deflections and additional degrees-of-freedom. A low part count and relatively large minimum feature size can be scaled to the millimeter size while maintaining function and performance.

The L-Arm has two degrees-of-freedom (DoF), one wrist and one gripping. The jaws pivot independently about the same axis of rotation. Figure 2 shows the L-Arm with one jaw labeled. The pulley and jaw are rigidly connected and can be made as one part. The flexure connects the jaw to the ground link (which is connected to the instrument shaft). The second jaw is identical to the first and is rotated 180 deg so the jaws face each other. A side view schematic of a single jaw is shown in Fig. 3. The moment arm for the cables is determined by the pulley radius, R. The approximate center of rotation is labeled CoR. F_{IN_1} and F_{IN_2} are each a combination of preload and actuation forces.

[1]Corresponding author.

Manuscript received July 25, 2016; final manuscript received March 5, 2017; published online June 27, 2017. Assoc. Editor: Carl Nelson.

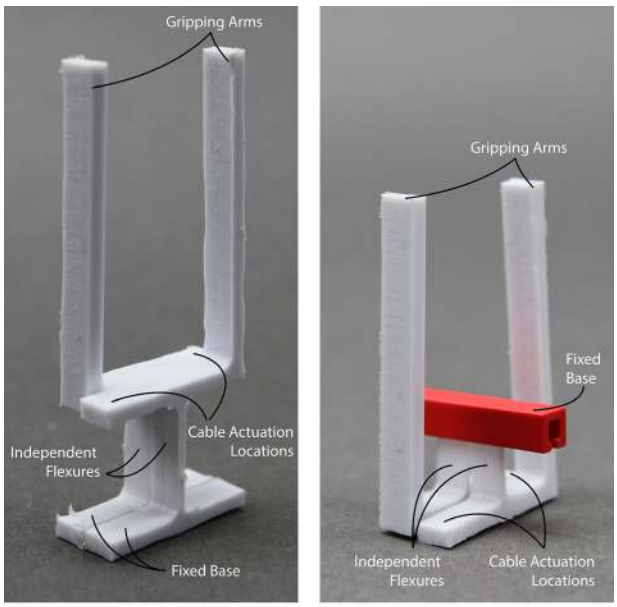

Fig. 1 (*a*) L-Arm and (*b*) inverted L-Arm polypropylene prototypes

2.1 Addressing Compressive Loads. Most robotic minimally invasive surgical instrument designs locate the end effector at the distal end of a long shaft. Cables extending the length of the shaft actuate the instrument and also induce a compressive preload on the system. Conventional compliant mechanisms often have low resistance to compressive loading and may buckle if the compressive load is too high. Inverting compliant mechanisms can enable them to support high compressive loads and has been studied previously [3]. This principle of inversion was applied to the L-Arm design as shown in Fig. 1(*b*). The inversion of flexures in the L-Arm mechanism eliminates the occurrence buckling by placing the flexible members normally in compression in tension. Note that a load causing the flexures to be in compression in Fig. 1(*a*) would result in tensile loading of the flexures in Fig. 1(*b*). In Fig. 1(*a*), the mechanism consists of, from bottom to top, a base or ground, flexures, and L-shaped jaws. As a downward actuation force is applied to either extreme of the horizontal segment of the L-shaped jaw, the respective flexure is placed in compression. In Fig. 1(*b*), the inverted mechanism consists of, from bottom to top, the L-shaped jaws, flexures, and ground link (labeled "fixed base"). As a downward actuation force is applied to either extreme of the horizontal segment of the L-shaped jaw, the respective flexure is placed in tension. In this way, the first challenge of inadequate performance in compression is overcome.

2.2 Addressing Stresses Due to Large Deformations. There are three fundamental ways to modify a flexure's stiffness (and therefore control stresses): geometry, boundary conditions, and material properties. These three ways can be varied independently to tailor a compliant flexure for a specific application.

While the large-scale proof-of-concept 38-mm L-Arm prototypes described in this paper (see Fig. 2) were created with flexures consisting of two wires placed side by side, it is expected that the flexures in the 3 mm L-Arm design will have a rectangular

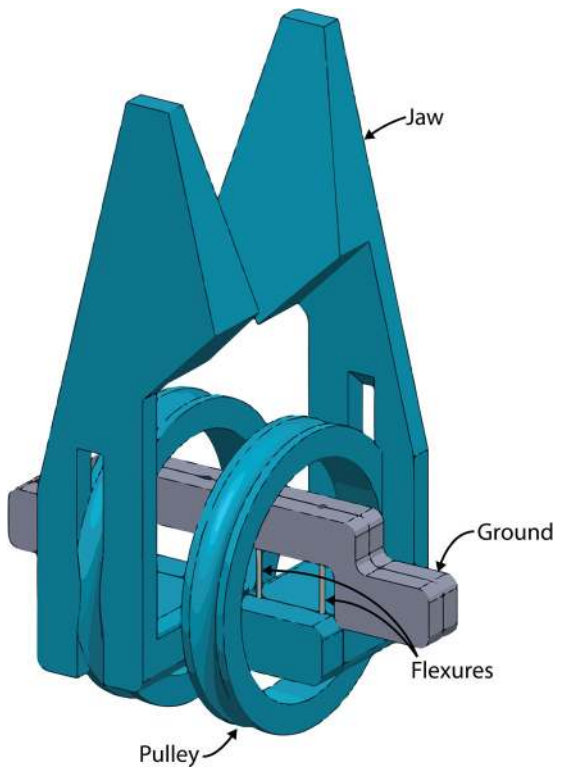

Fig. 2 Inverted L-Arm with NiTi wire flexures. While both identical jaws are shown, only one has been labeled.

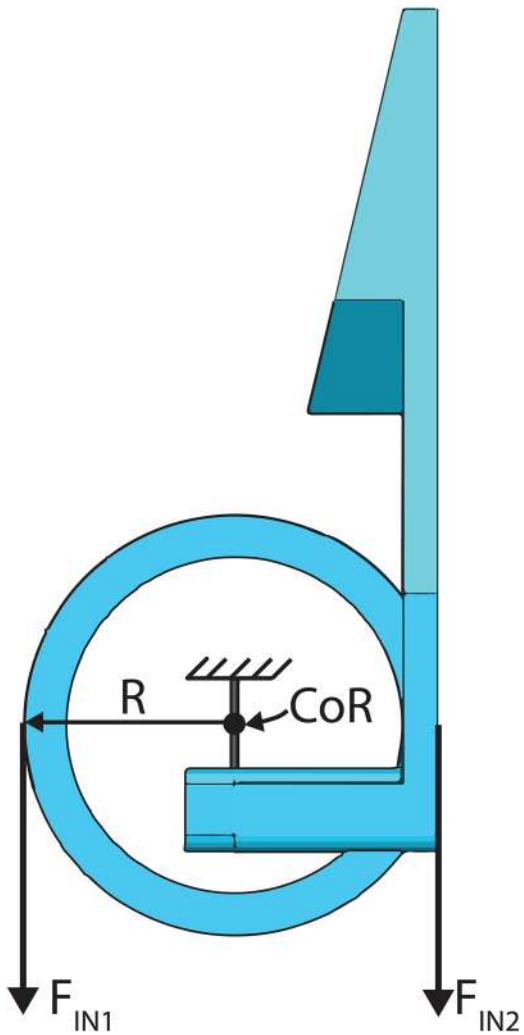

Fig. 3 A single jaw of the L-Arm compliant mechanism is viewed from the side. *R* is the moment arm length (radius of the pulley), CoR is the approximate center of rotation, and F_{IN_1} and F_{IN_2} are input forces provided by cables.

cross section. The following discussion on flexure geometry assumes a rectangular cross section.

The L-Arm flexure geometry was designed to minimize bending stress while still providing adequate strength in tensile loading. To this end, the thickness of the flexures was decreased to enable higher angular deflection before reaching the limiting bending stress. The flexure width was kept as large as possible to provide lateral and torsional stability.

The flexible members of the L-Arm were designed using the pseudorigid-body model with the small-length flexural pivot (SLFP) assumption, which is that if the flexure length is small compared to the rigid portion of the mechanism, the center of rotation of the mechanism can be approximated as the midpoint of the flexure along its length. The SLFP assumption is valid when the flexible member length, l, is much less than the overall length, L, of the mechanism ($l \ll L$) [2].

The SLFP assumption simplifies the kinematic analysis of the mechanism to that of a simple pin joint with rigid links. The jaw faces were designed such that the plane in which each face lies passes through the axis of rotation of the flexures. When in the closed position, the jaw faces make complete contact with each other. Note that the compliant nature of the mechanism enables the contact profile of the jaws to be tailored for a specific task or procedure. The actuation pulleys were also designed with their axes of rotation aligned with those of their respective flexure.

The L-Arm flexure has boundary conditions where one side of the flexure is fixed to ground while the other side is fixed to the moving jaw. These boundary conditions are also part of the SLFP assumption.

Several materials were identified as possible candidates for the flexure including stainless steel, titanium, metallic glass, and the nickel titanium alloy nitinol (NiTi). These materials were selected for their favorable compliant characteristics, including a relatively large S_y/E, as well as biocompatibility [12–14]. NiTi consists of nearly equal atomic percentages of nickel and titanium. NiTi can exhibit the superelastic effect and is therefore of interest in the field of compliant mechanisms due to the large strains that it can undergo before yielding. It can reach strains of 6–8% with very small material set, while steels generally reach strains on the order of less than 1% before yielding.

Analysis determined that a stainless steel flexure could undergo angular deflections of <30 deg for a given geometry before yielding. A metallic glass flexure was designed that could deflect to $\sim$45 deg [15]. NiTi was investigated for its ability to undergo large strains before yielding and was ultimately chosen as the flexure material due to its potentially large range of motion.

The selection of superelastic NiTi as the flexure material overcame the second challenge and enabled the L-Arm mechanism to reach the large deflections required in MIS instruments.

2.3 Addressing Variable Mechanical Advantage. The third challenge encountered with early L-Arm concepts (see Fig. 1) was a variable actuation moment arm that tended to zero as the mechanism was deflected. Once the effective length of the actuation moment arm reached zero, the L-Arm could not be deflected farther even if the flexure itself was designed for greater angular deflections.

To overcome this challenge, a pulley was integrated into each gripper jaw to maintain a constant moment arm for the cables as the mechanism is actuated. The cable is fixed at the top of the pulley and routed over each side. Figure 3 shows the pulley geometry. The forces F_{IN_1} and F_{IN_2} are transmitted from the back (proximal) end of the instrument to the L-Arm mechanism via the cables. The cables are placed in opposing pairs because they only transmit tensile forces. The pulley and jaw can be made as one piece, reducing the mechanism part count and simplifying the manufacturing process. The circular pulley was designed with its center at the midpoint of the flexure. Using the SLFP assumption, this is also the approximate center of rotation of the jaw. While the resulting mechanical advantage is not constant, the variability is significantly reduced. The integrated pulley enables angular deflections exceeding ± 90 deg for each jaw to be achieved using cable actuation.

A mechanical advantage analysis was completed to compare the L-Arm with and without the integrated pulley. A labeled diagram of one jaw of the L-Arm without a pulley used in the analysis is shown in Fig. 4. A diagram of the L-Arm with a pulley is shown in Fig. 5. Using the values in Table 1, the mechanical advantage for the L-Arm with and without the integrated pulley was calculated as a function of angular deflection. Figure 6 shows the mechanical advantage for a 3 mm L-Arm with and without a pulley. Titanium was used for simplicity in the model. The material modulus of elasticity will only affect the shape of the curve, not the point at which the mechanical advantage becomes negative (for the L-Arm without a pulley). The point at which the curve crosses zero is dictated by the effective moment arm for the input force, F_{IN}. The plot also shows that the mechanical advantage of the L-Arm design with a pulley has less variation compared to the L-Arm without a pulley and it never becomes negative. For the chosen geometry, the L-Arm without a pulley can be actuated via cables up to $\sim$65 deg before the mechanical advantage reaches zero. The L-Arm design with a pulley can be cable-actuated over the desired range of motion, ± 90 deg. Although the mechanical advantage is much less than 1 for both designs, it is not anticipated as a problem for robotic MIS instruments driven by powerful electric motors that can develop the torques necessary to obtain the desired output force at the tip of the instrument. Current commercial instrument architectures have similar mechanical advantages as the L-Arm concept. In this case, a 2 N output force was used as the working load for a 3-mm surgical instrument.

3 Large-Scale Proof-of-Concept Prototype

Multiple rounds of prototyping and mathematical modeling were used to verify that the strategies outlined in this work could

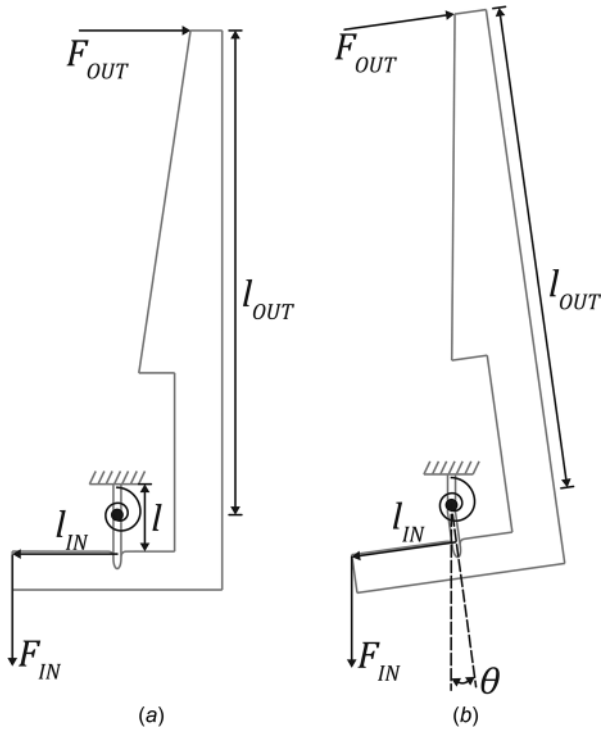

Fig. 4 Model used in the mechanical advantage analysis of the L-Arm gripper mechanism without a pulley. Note that F_{OUT} is modeled as a follower force while F_{IN} is modeled as a vertical force. The location at which F_{IN} is applied changes relative to the approximate center of rotation as the mechanism is actuated.

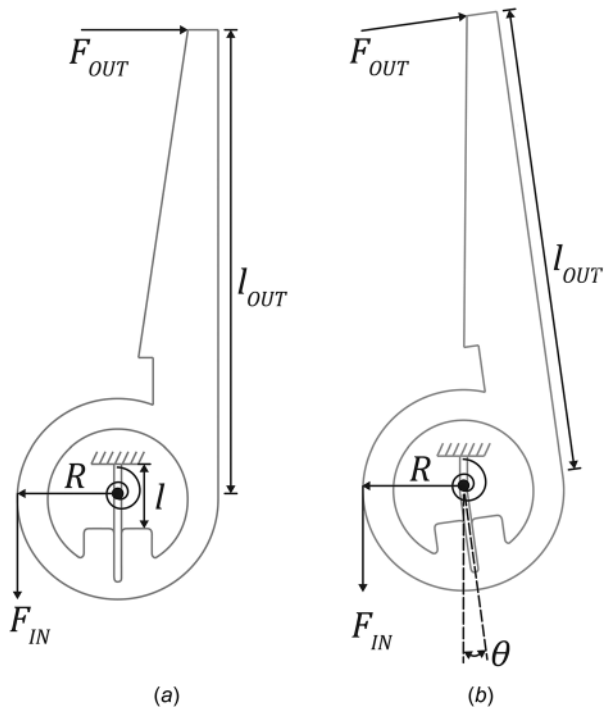

Fig. 5 Model used in the mechanical advantage analysis of the L-Arm gripper mechanism with a pulley integrated into the jaw. Note that F_{OUT} is modeled as a follower force while F_{IN} is modeled as a vertical force. The location at which F_{IN} is applied does not change relative to the approximate center of rotation as the mechanism is actuated.

Table 1 Values used in the mechanical advantage analysis of a 3-mm L-Arm mechanism

Dimension	Value
l	1.25 mm
h	0.102 mm
b	0.7 mm
l_{IN}	1.299 mm
l_{OUT}	7.0 mm
R	1.299 mm
E	113.8 GPa
F_{OUT}	2.0 N

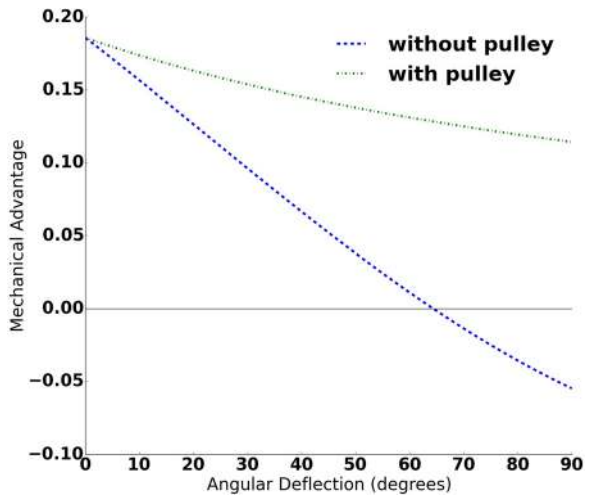

Fig. 6 Mechanical advantage plotted against angular deflection (in deg) for a 3-mm L-Arm using the values listed in Table 1

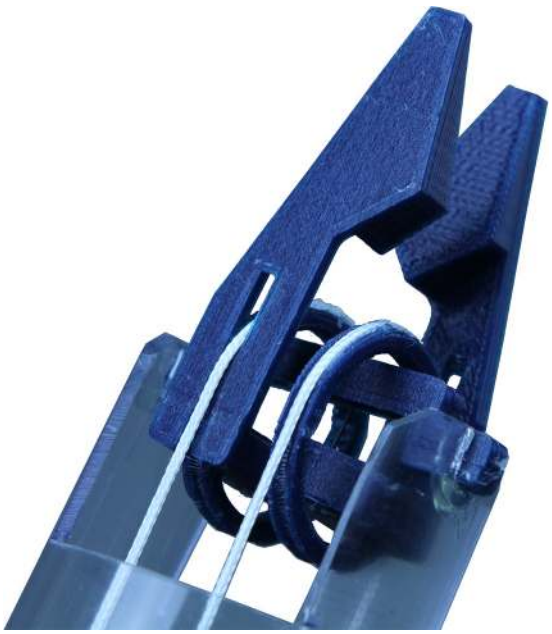

Fig. 7 Thirty eight millimeter proof-of-concept prototype of the inverted L-Arm with NiTi wire flexures

enable feasible compliant mechanisms capable of the desired performance (2DoF and an angular deflection ±90 deg, as well as the ability to perform gripping and lifting functions). A large-scale proof-of-concept prototype was constructed to test the inverted L-Arm concept. The jaws and ground link were made of polylactic acid using an additive manufacturing process. The actuation cables were made using 0.84-mm polyester twine. The shaft tube was a 38-mm clear cellulose tube. The flexures were made using 0.38-mm (0.015 in) diameter superelastic NiTi wire. The flexures

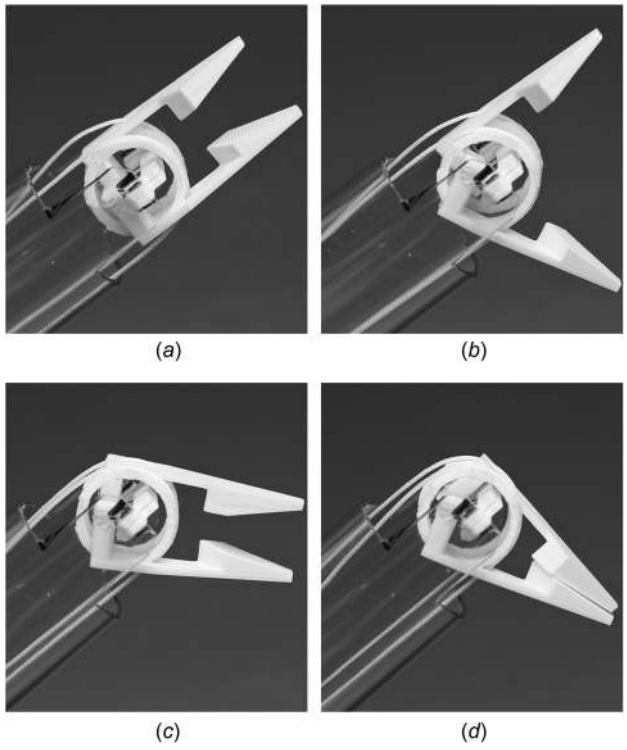

Fig. 8 Thirty eight millimeter L-Arm prototype showing independent actuation of each jaw as well as the gripping function of the mechanism

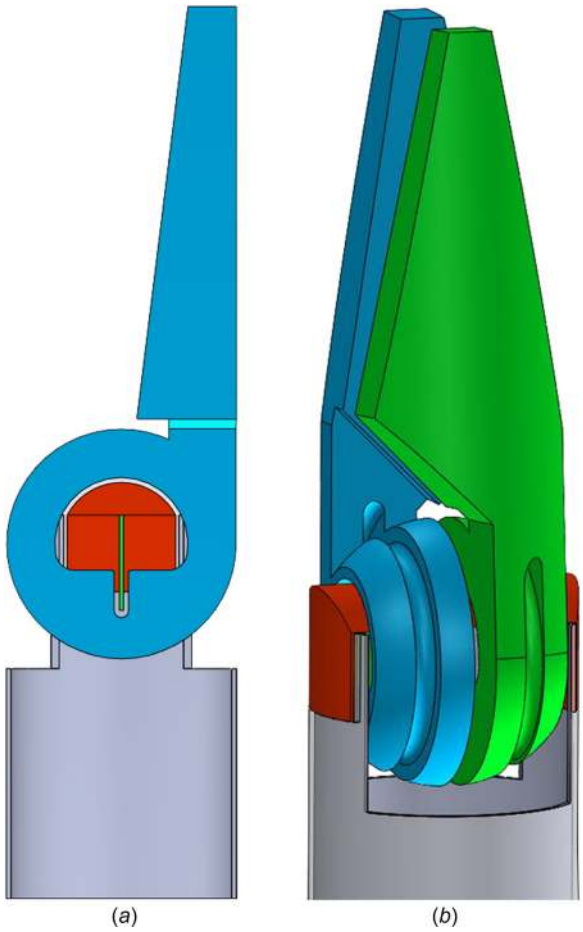

Fig. 9 Six millimeter L-Arm model: (*a*) shows a section view with the jaw, the thin NiTi flexure, and the fixed portion concentric to the jaw and (*b*) is a model of the assembled mechanism

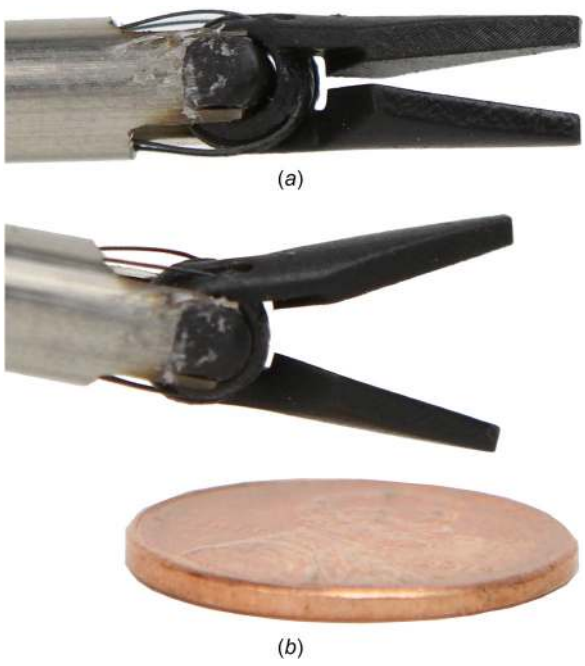

Fig. 10 Six millimeter L-Arm SLA prototype with NiTi flexures: (*a*) shows the nominal state and (*b*) shows one jaw in a deflected state. U.S. penny for scale.

are ~5 mm in length. Two wires were placed side by side at a distance of 5 mm to create the flexure for each jaw. The torsional stiffness (about an axis parallel to the instrument shaft axis) of the jaws is increased by moving the two NiTi wires apart from each other. The prototype is shown in Figs. 7 and 8.

The jaws are independently actuated via the cables. The prototype was able to undergo ±90 deg from the undeflected position without yielding, and demonstrated the ability to perform gripping and lifting functions. The lifting function consisted of gripping an object, lifting it, and moving it to a new location supported by only the gripper mechanism.

4 Three Millimeter and 6 mm L-Arm Designs

Three millimeter and 6 mm mechanisms were modeled and prototyped (see Fig. 9). Jaws and ground links for 3 mm and 6 mm prototypes were made using a stereolithography (SLA) additive manufacturing process. The 6 mm parts were assembled with NiTi flexures to create a 6 mm prototype.

4.1 Three Millimeter and 6 mm Prototypes. Parts for a 3 mm prototype were created using an SLA process. A more robust 6 mm SLA prototype was also created (see Fig. 10). These prototypes demonstrate that the minimum feature size of the 3 mm and 6 mm designs can be achieved with current commercial technologies. The 6 mm prototype also verified that the design was able to be assembled.

5 Conclusion

This work addressed the three challenges of employing compliant mechanisms as grippers in cable-actuated minimally invasive surgery instruments: compressive loading, maximum angular deflection, and a variable actuation moment arm. These issues were resolved by inverting the mechanism, designing appropriate geometry and boundary conditions, employing NiTi flexures, and integrating a pulley into each jaw. The angular rotation is predicted to be at least ±90 deg.

The 3-mm L-Arm concept as designed has a total of six parts, four of which are unique. A lower part count compared to commercially available instruments could reduce cost and improve the availability of MIS procedures for a broad range of patients [16].

The inverted L-Arm compliant mechanism is a good candidate for a 3-mm 2DoF minimally invasive surgical instrument. A third degree-of-freedom could be added by locating an existing 1DoF wrist mechanism with an axis of rotation orthogonal to the axis of rotation of the L-Arm below the end effector.

The principles and strategies developed here may prove useful in creating other compliant mechanism surgical instruments [17].

Acknowledgment

The financial support provided by Intuitive Surgical, Inc., is gratefully acknowledged. This material is partially based on work supported by the National Science Foundation and the Air Force Office of Scientific Research under NSF Grant No. EFRI-ODI-SSEI-1240417.

References

[1] Antoniou, S. A., Antoniou, G. A., Antoniou, A. I., and Granderath, F.-A., 2015, "Past, Present, and Future of Minimally Invasive Abdominal Surgery," JSLS: J. Soc. Laparoendoscopic Surg., **19**(3), pp. 52–54.
[2] Howell, L. L., 2001, *Compliant Mechanisms*, Wiley, New York.
[3] Guérinot, A. E., Magleby, S. P., Howell, L. L., and Todd, R. H., 2005, "Compliant Joint Design Principles for High Compressive Load Situations," ASME J. Mech. Des., **127**(4), pp. 774–781.
[4] Jelínek, F., Arkenbout, E. A., Henselmans, P. W., Pessers, R., and Breedveld, P., 2015, "Classification of Joints Used in Steerable Instruments for Minimally Invasive Surgery—A Review of the State of the Art," ASME J. Med. Devices, **9**(1), p. 010801.
[5] Liu, J., Hall, B., Frecker, M., and Reutzel, E. W., 2013, "Compliant Articulation Structure Using Superelastic Nitinol," Smart Mater. Struct., **22**(9), p. 094018.

[6] York, P. A., Swaney, P. J., Gilbert, H. B., and Webster, R. J., III, 2015, "A Wrist for Needle-Sized Surgical Robots," IEEE International Conference on Robotics and Automation (ICRA), Seattle, WA, May 26–30, pp. 1776–1781.
[7] Awtar, S., Trutna, T. T., Nielsen, J. M., Abani, R., and Geiger, J., 2010, "Flexdex™: A Minimally Invasive Surgical Tool With Enhanced Dexterity and Intuitive Control," ASME J. Med. Devices, **4**(3), p. 035003.
[8] Cronin, J. A., Frecker, M. I., and Mathew, A., 2008, "Design of a Compliant Endoscopic Suturing Instrument," ASME J. Med. Devices, **2**(2), p. 025002.
[9] Aguirre, M., Steinórsson, Á. T., Horeman, T., and Herder, J., 2015, "Technology Demonstrator for Compliant Statically Balanced Surgical Graspers," ASME J. Med. Devices, **9**(2), p. 020926.
[10] Bhargav, S. D., Chakravarthy, S., and Ananthasuresh, G., 2012, "A Compliant End-Effector to Passively Limit the Force in Tele-Operated Tissue-Cutting," ASME J. Med. Devices, **6**(4), p. 041005.
[11] Edmondson, B. J., Bowen, L. A., Grames, C. L., Magleby, S. P., Howell, L. L., and Bateman, T. C., 2013, "Oriceps: Origami-Inspired Forceps," ASME Paper No. SMASIS2013-3299.
[12] Calin, M., Gebert, A., Ghinea, A. C., Gostin, P. F., Abdi, S., Mickel, C., and Eckert, J., 2013, "Designing Biocompatible Ti-Based Metallic Glasses for Implant Applications," Mater. Sci. Eng.: C, **33**(2), pp. 875–883.
[13] Ryhänen, J., Niemi, E., Serlo, W., Niemelä, E., Sandvik, P., Pernu, H., and Salo, T., 1997, "Biocompatibility of Nickel-Titanium Shape Memory Metal and Its Corrosion Behavior in Human Cell Cultures," J. Biomed. Mater. Res., **35**(4), pp. 451–457.
[14] Haider, W., and Munroe, N., 2011, "Assessment of Corrosion Resistance and Metal Ion Leaching of Nitinol Alloys," J. Mater. Eng. Perform., **20**(4–5), pp. 812–815.
[15] Tanner, J. D., 2014, "Design and Analysis of Robotically-Controlled Minimally Invasive Surgical Instruments," Master's thesis, Brigham Young University, Provo, UT.
[16] Grames, C. L., Tanner, J. D., Jensen, B. D., Magleby, S. P., Steger, J. R., and Howell, L. L., 2015, "A Meso-Scale Rolling-Contact Gripping Mechanism for Robotic Surgery," ASME Paper No. DETC2015-46516.
[17] Dearden, J. L., 2016, "Design and Analysis of Two Compliant Mechanism-Based Instruments for Minimally Invasive Surgery," Master's thesis, Brigham Young University, Provo, UT.